

Iron-57 Nuclear Shieldings as a Quantitative Tool for Estimating Porphyrin Ruffling in Hexacoordinated Carbonmonoxy Heme Model Compounds in Solution

Charalampos G. Kalodimos,[†] Ioannis P. Gerothanassis,^{*,†} Eric Rose,[‡] Geoffrey E. Hawkes,[§] and Roberta Pierattelli^{||}

Contribution from the Section of Organic Chemistry and Biochemistry, Department of Chemistry, University of Ioannina, Ioannina GR-45110, Greece, Laboratoire de Synthèse Organique et Organométallique, Université P. et M. Curie, UMR CNRS 7611, 4 Place Jussieu, 75252 Paris Cedex 05, France, Department of Chemistry, Queen Mary and Westfield College, University of London, Mile End Road, London E1 4NS, U.K., and Department of Chemistry, University of Florence, Via G. Capponi 7, 50121 Florence, Italy

Received November 9, 1998. Revised Manuscript Received February 1, 1999

Abstract: ⁵⁷Fe NMR spectra of several carbonmonoxy hemoprotein models with varying polar and steric effects of the distal organic superstructure, constraints of the proximal side, and porphyrin ruffling are reported. ⁵⁷Fe shieldings, $\delta(^{57}\text{Fe})$, vary by nearly 900 ppm among various hemes, and an excellent correlation was found between $\delta(^{57}\text{Fe})$ and the absolute crystallographic average displacement of the meso carbon atoms, $|C_m|$, relative to the porphyrin core mean plane. The great variation of $\delta(^{57}\text{Fe})$ as a function of $|C_m|$ (~ 140 ppm/0.1 Å) demonstrates that iron-57 shieldings can be used in structure refinement protocols for the extraction of more accurate structures for heme rings in heme model compounds. The excellent correlation between iron-57 shieldings and the average shieldings of the meso carbons of the porphyrin skeleton of TPP derivatives suggests that the two probes reflect similar types of electronic and structural perturbations, which are primarily due to porphyrin ruffling. The present findings also emphasize the value in predicting ⁵⁷Fe shieldings in superstructured metalloporphyrins from ¹³C shieldings of the meso carbons.

Introduction

Tetrapyrrole derivatives, including porphyrins, are found as cofactors in a bewildering array of proteins. Their important functions include O₂ transport (hemoglobins) and storage (myoglobins), oxygen reduction (oxidases), electron transfer (cytochromes), a large number of other enzymatic reactions (peroxidases, catalases, cytochromes P-450, methyltransferases, etc.), conversion of solar energy to chemical energy (photosynthetic reaction centers), etc.¹ It has been recognized in the last 10 years that the hemes in many hemoproteins are highly distorted from planarity, contrary to early X-ray crystal structures in which the heme was constrained to a planar conformation during the refinement procedure.^{1,2} The type of distortion differs for proteins with different functions, and the types of distortion are conserved for proteins isolated from various species. Currently, attempts have been made to determine whether these nonplanar porphyrin distortions in proteins have functional

significance and to determine the mechanism by which nonplanarity influences activity.

The importance of nonplanar distortions of the heme is also emphasized by recent studies of heme model compounds. It has been suggested that the nonplanar structure of the heme influences chemical and photophysical properties such as axial ligand affinity, redox potentials, chirality, basicity, metalation rate, excited-state lifetimes, transition dipoles, and energies.^{2,3}

One of the most significant type of porphyrin distortion is the so-called ruffling. A porphyrin is ruffled when opposite pyrrole rings are counterrotated so that the meso carbon atoms (C_{meso}) of each pyrrole ring are alternately displaced above and below the mean porphyrin plane.⁴ Structural data on heme proteins reveal that ruffling of hemes is common in nature;

- (3) (a) Grodzicki, M.; Flint, H.; Winkler, H.; Walker, F. A.; Trautwein, A. X. *J. Phys. Chem. A* **1997**, *101*, 4202–4207. (b) Cheng, B.; Munro, O. Q.; Marques, H. M.; Scheidt, W. R. *J. Am. Chem. Soc.* **1997**, *119*, 10732–10742. (c) Munro, O. Q.; Bradley, J. C.; Hancock, R. D.; Marques, H. M.; Marsicano, F.; Wade, P. W. *J. Am. Chem. Soc.* **1992**, *114*, 7218–7230. (d) Senge, M. O.; Kalisch, W. W. *Inorg. Chem.* **1997**, *36*, 6103–6116. (e) Munro, O. Q.; Marques, H. M.; Debrunner, P. G.; Mohanrao, K.; Scheidt, W. R. *J. Am. Chem. Soc.* **1995**, *117*, 935–954. (f) Safo, M. K.; Walker, F. A.; Raitsimring, A. M.; Walters, W. P.; Dolata, D. P.; Debrunner, P. G.; Scheidt, W. R. *J. Am. Chem. Soc.* **1994**, *116*, 7760–7770. (g) Song, X.-Z.; Jentzen, W.; Jia, S.-L.; Jaquinod, L.; Nurco, D. J.; Medforth, C. J.; Smith, K. M.; Shelnut, J. A. *J. Am. Chem. Soc.* **1996**, *118*, 12975–12988. (h) Drain, C. M.; Gentemann, S.; Roberts, J. A.; Nelson, N. Y.; Medforth, C. J.; Jia, S.; Simpson, M. C.; Smith, K. M.; Fajer, J.; Shelnut, J. A.; Holten, D. *J. Am. Chem. Soc.* **1998**, *120*, 3781–3791. (i) Cheng, R.-J.; Chen, P.-Y.; Gau, P.-R.; Chen, C.-C.; Peng, S.-M. *J. Am. Chem. Soc.* **1997**, *119*, 2563–2569. (j) Vitols, S. E.; Roman, J. S.; Ryan, D. E.; Blackwood, M. E., Jr.; Spiro, T. G. *Inorg. Chem.* **1997**, *36*, 764–769.
- (4) Scheidt, W. R.; Lee, Y. J. *Struct. Bonding* **1987**, *64*, 1–72.

* To whom correspondence should be addressed. Tel: (0651) 98389. Fax: (0651) 45840. E-mail: igeroth@cc.uoi.gr.

[†] University of Ioannina.

[‡] Université P. et M. Curie.

[§] University of London.

^{||} University of Florence.

(1) (a) Shelnut, J. A.; Song, X.-Z.; Ma, J.-G.; Jia, S.-L.; Jentzen, W.; Medforth, C. J. *Chem. Soc. Rev.* **1998**, *27*, 31–41. (b) Walker, F. A.; Simonis, U. In *Encyclopedia of Inorganic Chemistry*; King, R. B., Ed.; Wiley: New York, 1994; pp 1785–1846. (c) Milgrom, L. R. *The Colours of Life*; Oxford University Press: New York, 1997.

(2) (a) Jentzen, W.; Ma, J.-G.; Shelnut, J. A. *Biophys. J.* **1998**, *74*, 753–763. (b) Ma, J.-G.; Laberge, M.; Song, X.-Z.; Jentzen, W.; Jia, S.-L.; Zhang, J.; Vanderkooi, J. M.; Shelnut, J. A. *Biochemistry* **1998**, *37*, 5118–5128.

myoglobin–CO exhibits an almost flat porphyrin,⁵ while in carbonyl hemoglobin the porphyrin is clearly ruffled.⁶

Currently, a few spectroscopic techniques for distinguishing the magnitude of nonplanar distortions have been suggested including UV–visible, resonance Raman, and IR spectroscopy.^{1,3,7} Iron porphyrin complexes, however, have not been investigated sufficiently. Many questions remain as to whether the spectroscopic markers of nonplanar conformation, primarily deduced for nickel porphyrin complexes, can be readily used for iron porphyrins. Recently, we showed the great potential of the shieldings of meso carbons in structural studies of porphyrin distortion in superstructured heme model compounds in solution.⁸ Despite its significance, this relationship cannot be extended to other porphyrins which are not TPP⁹ derivatives as, for example, in Mb and Hb. Therefore, improved spectroscopic probes of porphyrin structure are needed to characterize the different distortions for a wide range of environments and porphyrin derivatives.

There has been increasing interest in the use of ⁵⁷Fe NMR as a probe of heme protein structure since iron is a central element of all heme proteins and the extremely large ⁵⁷Fe chemical shift range (~12 000 ppm) offers a very sensitive and direct probe of the electron density and asymmetry at the iron atom.^{10–13} The low natural abundance of ⁵⁷Fe (2.2%) is readily remedied by isotopic enrichment, and recent studies on heme models suggest that spin–lattice relaxation may be reasonably efficient via the chemical shift anisotropy mechanism. Baltzer and Landergren have previously indicated that ⁵⁷Fe NMR chemical shifts of heme models vary by more than 600 ppm and in a seemingly regular fashion, giving a low-frequency shift with increased ruffling of the porphyrin geometry.^{13a} In the present work, we have pursued ⁵⁷Fe NMR studies of a series of six-coordinated heme model compounds (95% ⁵⁷Fe enriched)

(5) Yang, F.; Phillips, G. N., Jr. *J. Mol. Biol.* **1996**, *256*, 762–774.

(6) Derewenda, Z.; Dodson, G.; Emsley, P.; Harris, D.; Nagai, K.; Perutz, M.; Reynaud, J.-P. *J. Mol. Biol.* **1990**, *211*, 515–519.

(7) (a) Blackwood, M. E., Jr.; Rush, T. S., III; Medlock, A.; Dailey, H. A.; Spiro, T. G. *J. Am. Chem. Soc.* **1997**, *119*, 12170–12174. (b) Jentzen, W.; Simpson, M. C.; Hobbs, J. D.; Song, X.; Ema, T.; Nelson, N. Y.; Medforth, C. J.; Smith, K. M.; Veyrat, M.; Mazzanti, M.; Ramasseul, R.; Marchon, J.-C.; Takeuchi, T.; Goddard, W. A., III; Shelnutz, J. A. *J. Am. Chem. Soc.* **1995**, *117*, 11085–11097.

(8) Kalodimos, C. G.; Gerotheranassis, I. P. *J. Am. Chem. Soc.* **1998**, *120*, 6407–6408.

(9) Abbreviations: TPP, tetraphenylporphyrin; 1-MeIm, 1-methylimidazole; 1,2-diMeIm, 1,2-dimethylimidazole; 1-BuIm, 1-butylimidazole; **A**, $\alpha,\alpha-5,15-[2,2'-(\text{dodecanediamido})\text{diphenyl}]-\alpha,\alpha-10,20\text{-bis}(o\text{-pivaloylamidophenyl})\text{porphyrin}$; **B**, $\alpha,\alpha-5,15-[2,2'-(\text{decane-diamido})\text{diphenyl}]-\alpha,\alpha-10,20\text{-bis}(o\text{-pivaloylamidophenyl})\text{porphyrin}$; **C**, $\alpha,\alpha-5,15-[2,2'-(\text{octanediamido})\text{diphenyl}]-\alpha,\alpha-10,20\text{-bis}(o\text{-pivaloylamidophenyl})\text{porphyrin}$; **D**, $\alpha,\alpha-5,10,15-[1,3,5\text{-benzenetriyltriacetyltris}(o\text{-aminophenyl})]-\alpha-20\text{-}(o\text{-pivaloylamidophenyl})\text{-porphyrin}$; **E**, $\alpha,\alpha,\alpha-5,10,15,20\text{-[pyrromellitoyltetrakis}(o\text{-oxyethoxyphenyl})]\text{porphyrin}$; **F**, $\alpha,\alpha,\alpha-5,10,15,20\text{-tetrakis}(o\text{-pivaloylamidophenyl})\text{-porphyrin}$; **G**, $\alpha,\alpha-5,15-[2,2'-(\text{dodecanediamido})\text{diphenyl}]-\beta,\beta-10,20-[2,2'-(5\text{-imidazol-1-ylnonane-1,9-diamido})\text{diphenyl}]\text{porphyrin}$; **H**, tetraphenylporphyrin.

(10) (a) Polam, J. R.; Wright, J. L.; Christensen, K. A.; Walker, F. A.; Flint, H.; Winkler, H.; Grodzicki, M.; Trautwein, A. X. *J. Am. Chem. Soc.* **1996**, *118*, 5272–5276. (b) Mink, L. M.; Polam, J. R.; Christensen, K. A.; Walker, F. A. *J. Am. Chem. Soc.* **1995**, *117*, 9329–9339. (c) Mink, L. M.; Christensen, K. A.; Walker, F. A. *J. Am. Chem. Soc.* **1992**, *114*, 6930–6931.

(11) Gerotheranassis, I. P.; Kalodimos, I. P.; Hawkes, G. E.; Haycock, P. *J. Magn. Reson.* **1998**, *131*, 163–165.

(12) (a) Lee, H. C.; Gard, J. K.; Brown, T. L.; Oldfield, E. *J. Am. Chem. Soc.* **1985**, *107*, 4087–4088. (b) Chung, J.; Lee, H. C.; Oldfield, E. *J. Magn. Reson.* **1990**, *90*, 148–157. (c) McMahon, M. T.; deDios, A. C.; Godbout, N.; Salzmann, R.; Laws, D. D.; Le, H.; Havlin, R.; Oldfield, E. *J. Am. Chem. Soc.* **1998**, *120*, 4784–4797. (d) Havlin, R.; Salzmann, R.; Dedrunner, P. G.; Oldfield, E. *J. Phys. Chem. A* **1998**, *102*, 2342–2350.

(13) (a) Baltzer, L.; Landergren, M. *J. Am. Chem. Soc.* **1990**, *112*, 2804–2805. (b) Baltzer, L.; Becker, E. D.; Tschudin, R. G.; Gansow, O. A. *J. Chem. Soc., Chem. Commun.* **1985**, 1040–1041. (c) Baltzer, L. *J. Am. Chem. Soc.* **1987**, *109*, 3479–3481.

(Figure 1) with varying polar and steric effects due to the distal organic superstructure, constraints of the proximal side and degree of porphyrin distortion with the purpose of further establishing ⁵⁷Fe shieldings as an extremely sensitive and quantitative probe for studying nonplanar distortions of porphyrins in solution.

Experimental Section

The porphyrin complexes were synthesized as described previously.¹⁴ ⁵⁷Fe₂O₃ (95% enriched in ⁵⁷Fe) was then used for the iron insertion according to the procedure of Landergren and Baltzer.¹⁵ A small excess of iron (twice the molar amount of porphyrin) was used to make the insertion quantitative. The incorporation of iron was monitored by measurement of the electronic absorption spectra of the solution. After deoxygenation by flushing a dichloromethane solution with pure argon, the samples were reduced to the iron(II) form using aqueous sodium dithionite solution. After separation of the two phases, the organic layer was transferred under argon into a second vessel containing an excess of 1-MeIm or 1,2-diMeIm. Separation of the aqueous phase and subsequent evaporation of the organic solvent resulted in a powder that was then loaded into a glass ampule which was connected to a vacuum pump and evacuated at room temperature for 3 h at a pressure of 10⁻⁴ Torr. The samples were dissolved in deuterated dichloromethane, and the solutions were transferred under argon into the NMR tubes (10 mm) via a stainless steel tube. CO under atmospheric pressure was then introduced to the ⁵⁷Fe(III) complexes to form the carbonylated derivatives, and the NMR tubes were sealed under a pressure of ~1 atm.

¹³C NMR spectra were obtained at 100.62 and 150.90 MHz with Bruker AMX-400 and AVANCE-600 instruments, respectively, equipped with high-resolution probes. The chemical shifts were determined relative to the resonance position of the solvent (CD₂Cl₂ ~53.8 ppm). ⁵⁷Fe NMR spectra were recorded at 19.58 MHz with a Bruker AMX-600 equipped with a 10 mm low-frequency multinuclear probe. The 90° pulse width, ~35 μ s, was determined on a saturated solution of ferrocene in toluene. Chemical shifts are reported with respect to Fe(CO)₅ at 0 ppm, using as a secondary standard a saturated solution of ferrocene in toluene ($\delta \approx 1531$ ppm).

Results and Discussion

The so-called “hybrid” porphyrins (Figure 1, **A–C**) consist of two pivalamido pickets on each side of an amide handle of variable length linked in a cross-trans configuration. Upon an increase in the steric hindrance by shortening the chain, CO affinities are decreased, indicating a steric discrimination against CO. However, X-ray structure determinations of these complexes reveal that the Fe–C–O unit is both linear and normal to the mean porphyrin plane.^{16,17} All contacts between the terminal oxygen atom and the aliphatic bridging chain are longer than 4 Å. The steric constraints are mainly released by a pronounced ruffling of the porphyrin macrocycle; the tighter the superstructure, the more ruffling. For complex **A**, the ⁵⁷Fe shielding, $\delta(^{57}\text{Fe})$, is 8036 ppm.^{13a} This model exhibits the smallest absolute crystallographic C_{meso} average perpendicular displacement, $|C_{\text{m}}|$, from the 24-atom mean porphyrin core in this series. When the chain is shortened, the degree of ruffling increases (C_{meso} average displacement is 0.29 and 0.44 Å for complexes **B** and **C**, respectively (Table 1)), resulting in a significant shielding of the ⁵⁷Fe resonance (7728 and 7735 ppm for complexes **B** and **C**, respectively). The ⁵⁷Fe NMR spectrum

(14) (a) Momenteau, M. In *Supramolecular Control of Structure and Reactivity*; Hamilton, A. D., Ed.; Wiley: New York, 1996; pp 155–223. (b) Momenteau, M. *Pure Appl. Chem.* **1986**, *58*, 1493–1502.

(15) Landergren, M.; Baltzer, L. *Inorg. Chem.* **1990**, *29*, 556–557.

(16) Ricard, L.; Weiss, R.; Momenteau, M. *J. Chem. Soc., Chem. Commun.* **1986**, 818–820.

(17) Tetreau, C.; Lavalette, D.; Momenteau, M.; Fischer, J.; Weiss, R. *J. Am. Chem. Soc.* **1994**, *116*, 11840–11848.

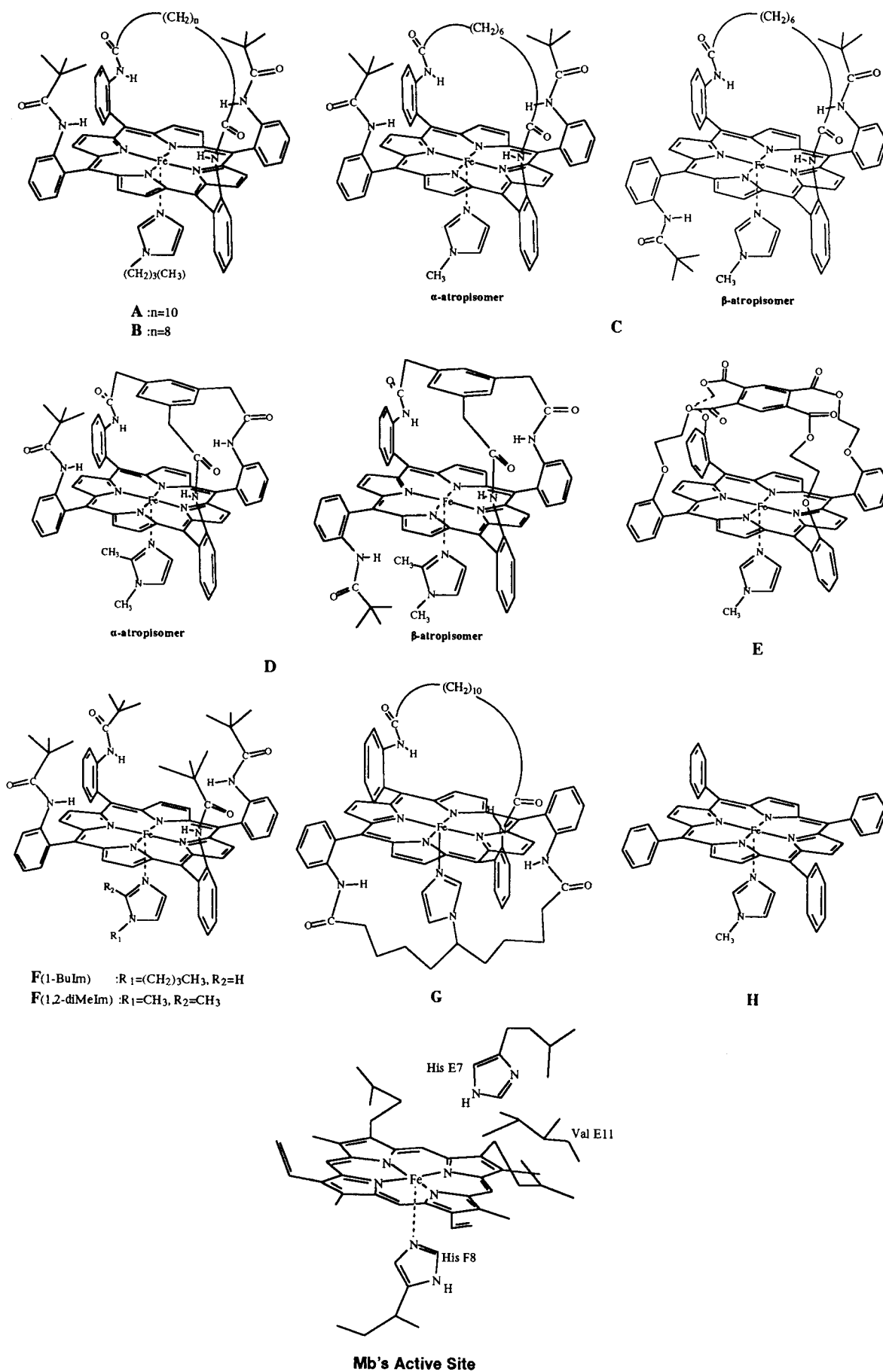


Figure 1. Schematic structures of the heme model compounds and the active site of Mb studied in this work.

Table 1. ^{57}Fe Shieldings, $\delta(^{57}\text{Fe})$, Average C_{meso} Shieldings, $\delta(^{13}\text{C}_{\text{m.av}})$, ^{13}C Shieldings of the Fe– ^{13}CO Unit, $\delta(^{13}\text{CO})^e$, and Significant Crystallographic Features for CO Binding of the Carbonylated Heme Model Compounds of Figure 1 and MbCO

compound	$\delta(^{57}\text{Fe})$ (ppm)	$\delta(^{13}\text{C}_{\text{m.av}})$ (ppm)	$\delta(^{13}\text{CO})^e$ (ppm)	$ C_{\text{m}} $ (Å)	Fe–C–O (deg)	Fe–C (Å)	Fe \cdots M l (Å)	Fe displ m (Å)
A	8036 ^c	114.4	205.0	0.155 ^f	180.0 ^f	1.728 ^f	8.43 ^f	0.02 ^f
B	7728 ^c	114.0	205.3	0.29 ^g	178.9 ^g	1.752 ^g	6.81 ^g	0.00 ^g
C α -atropisomer	7735	113.5	206.0	0.44 ^g	178.3 ^g	1.733 ^g	6.53 ^g	−0.06 ^g
β -atropisomer	7911	113.9	206.2					
D α -atropisomer	7400	112.8	204.6					
β -atropisomer	7560	113.0	204.7	0.53 ^h	172.5 ^h	1.768 ^h	5.36 ^h	0.01 ^h
E ^a conformer 1				0.04 ⁱ	172.9 ⁱ	1.742 ⁱ	5.57 ⁱ	0.02 ⁱ
conformer 2	8282	114.9	202.1	0.03 ^j	175.9 ^j	1.748 ^j	5.67 ^j	−0.01 ^j
F (1-BuIm)	8110 ^c	114.5	204.7					
F (1,2-diMeIm)	8099	114.5	205.0					
G ^b conformer 1	8207	114.6	203.9					
conformer 2	8199	114.6	204.3					
H	8195		205.0	0.03 ^j	179.3 ^j	1.793 ^j		−0.01 ^j
MbCO	8227 ^d		208.0	0.02 ^k	134 ^k	2.13 ^k		<0.1 ^k

^a There are two independent Fe(C_2 -Cap)(1-MeIm)(CO) molecules within the asymmetric part of the unit cell. ^b Two conformers which may be attributed to two forms of the model compound with two orientations of the axial imidazole which differ from each other by 180°. ^c Reference 13a. ^d Reference 12a. ^e Reference 22e. ^f Reference 16. ^g Reference 17. ^h Reference 18. ⁱ Reference 19. ^j Reference 20. ^k Reference 5. ^l Fe \cdots M is the distance between the centroid of distal cap or strap and the Fe atom; it defines the distal pocket size. ^m Fe deviation from the 24-atom plane; a positive value indicates displacement toward the CO group.

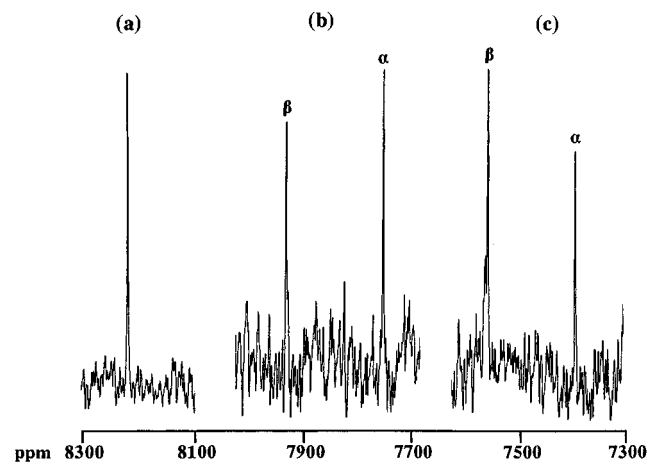


Figure 2. ^{57}Fe NMR chemical shift range for carbonylated heme models. Three representative spectra are shown: (a) **H**; (b) **C**; (c) **D**. α and β denote the α - and β -atropisomers, respectively. Conditions: saturated solutions in CD_2Cl_2 (≤ 20 mM), at 298 K; Bruker AMX-600 instrument, with $T_{\text{acq}} \sim 0.21$ s; 130 μs preacquisition delay to avoid acoustic ringing phenomena; sensitivity enhancement by a line-broadening function of 30 Hz; relaxation delay 20 ms; number of scans 30 000, 270 000, and 330 000 for (a), (b), and (c), respectively.

of model **C** indicates the presence of two resonances (Figure 2, Table 1) which can be attributed to α - and β -atropisomerization of one of the untethered picket which occurred during the iron insertion into the free base (this entailed the heating of the solution to 80 °C). Assignment of the α - and β -atropisomers, with relative integrals 1.4:1, was based on the NOE effect between the protons of the methyl groups of the “ β -picket” and the $-\text{N}-\text{CH}_3$ protons of the axial imidazole.

The superstructure of the “PocPiv” model (Figure 1, **D**) consists of a benzene cap attached to three out of four of the porphyrin phenyl substituents via *o*-amide linking groups and a fourth free pivalamido picket. The ^{57}Fe NMR spectrum indicates the presence of two resonances, with relative integrals 1:1.5, due to α - and β -atropisomerization of the untethered picket (Figure 2). The X-ray crystal structure of the β -atropisomer of **D** (in which the fourth picket is in the “down” position) shows the Fe–C–O angle to be 172.5°. The modest distortion

of the Fe–C–O unit is accompanied by considerable ruffling of the porphyrin periphery ($|C_{\text{m}}| = 0.53$ Å). Model **D** exhibits the most ruffled porphyrin plane among the compounds of Figure 1, and this is reflected in the ^{57}Fe resonance which is the most shielded (7560 ppm).

The “ C_2 -cap” model (Figure 1, **E**) consists of a 1,2,4,5-substituted benzene cap connected by four linkages of the type $-(\text{C}=\text{O})\text{O}(\text{CH}_2)_2\text{O}-$ to the ortho positions of the phenyl rings of the TPP. The refined X-ray structure shows the presence of two crystallographically independent porphyrin molecules with the Fe–C–O groups distorted from linearity (172.9 and 175.9°, Table 1).¹⁹ Only a single ^{57}Fe resonance is observed, which shows that the interconversion rate of the two conformers is, presumably, fast on the NMR time scale. Interestingly, the porphyrin ruffling is very small, and this results in a highly deshielded ^{57}Fe resonance (8282 ppm).

The simplest porphyrin studied in this work is TPP (Figure 1, **H**). A recent X-ray structure determination of the Fe^{II}TPP-(1-MeIm)CO complex shows that the Fe–C–O unit is both linear and normal to the mean porphyrin plane.²⁰ The degree of ruffling is very small ($|C_{\text{m}}|$ is only 0.03 Å), and the ^{57}Fe resonance is highly deshielded ($\delta(^{57}\text{Fe}) = 8195$ ppm).

When ^{57}Fe shieldings, $\delta(^{57}\text{Fe})$, are plotted against the absolute crystallographic average displacement of the C_{meso} relative to the porphyrin core mean plane, $|C_{\text{m}}|$, then a linear correlation is observed (Figure 3), which can be expressed as

$$\delta(^{57}\text{Fe}) \text{ (ppm)} = 8253.8 - 1337.9|C_{\text{m}}| \text{ (Å)} \quad (1)$$

with a correlation coefficient of 0.935. From this relationship it is evident that even small variations of porphyrin ruffling result in a significant change in ^{57}Fe shieldings which vary by ca. 720 ppm between the two extremes and in a regular fashion, giving a shielding with increased ruffling. Interestingly, Grodzicki and co-workers were the first to perform iron DFT calculations in porphyrins suggesting that ruffling of the porphyrin ring is a dominant factor in determining Mössbauer quadrupole splitting.^{3a}

Apart from that of TPP, the most striking type of distortion occurring in all of these models is ruffling. In TPP(1-MeIm)-

(19) Kim, K.; Ibers, J. A. *J. Am. Chem. Soc.* **1991**, *113*, 6077–6081.

(18) Kim, K.; Fettinger, J.; Sessler, J. L.; Cyr, M.; Hugdahl, J.; Collman, J. P.; Ibers, J. A. *J. Am. Chem. Soc.* **1989**, *111*, 403–405.

(20) Salzmann, R.; Ziegler, C. J.; Godbout, N.; McMahon, M. T.; Suslick, K. S.; Oldfield, E. *J. Am. Chem. Soc.* **1998**, *120*, 11323–11334.

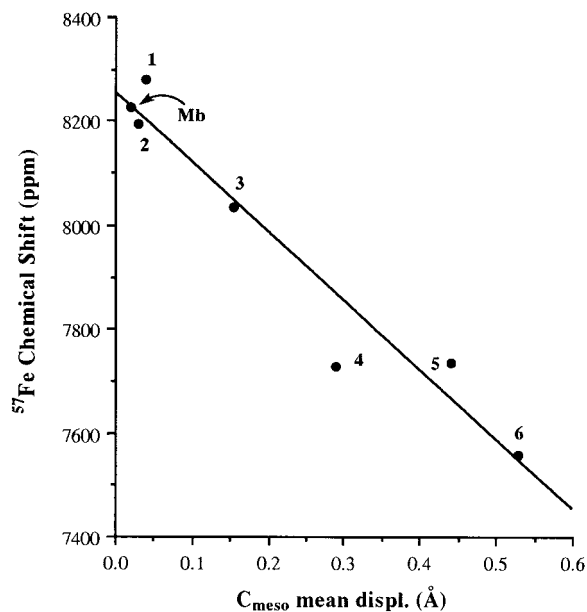


Figure 3. Plot of $\delta(^{57}\text{Fe})$ (ppm) vs $|C_m|$ (Å) for some of the heme model compounds of Figure 1 and Mb. Data points are as follows: 1, E; 2, H; 3, A; 4, B; 5, C α -atropisomer; 6, D β -atropisomer.

CO, the degree of ruffling is small, but it has a significant saddle distortion (C_β carbons are on average ~ 0.29 Å from the mean plane).²⁰ As can be seen in Figure 3, TPP fits very well the linear correlation, which means that saddling has only a minor effect on ^{57}Fe shieldings. Therefore, ^{57}Fe NMR spectroscopy proves to be an excellent means to distinguish ruffling from other types of porphyrin distortion. Furthermore, the great variation of $\delta(^{57}\text{Fe})$ as a function of $|C_m|$ (~ 140 ppm/0.1 Å) demonstrates that ^{57}Fe shieldings can be used in NMR structure refinement protocols for the extraction of more accurate structures for heme rings in model compounds. Interestingly, Oldfield and collaborators performed detailed quantum mechanical DFT calculations of ^{13}C , ^{17}O , and ^{57}Fe shieldings of metalloporphyrins and suggested that they can be used to predict, refine, and determine molecular structures.^{12c}

As has been already pointed out, the magnitudes of porphyrin substituent and solvent effects on ^{57}Fe shieldings of carbonylated hemes are substantially smaller than the ones encountered as the result of perturbations of the porphyrin core.^{13a} Thus, the above linear correlation could be extended to include results of hemoproteins. MbCO exhibits a very small degree of ruffling ($|C_m| = 0.02$ Å),⁵ and the ^{57}Fe signal appears at 8227 ppm.^{12a} As can be seen in Figure 3, MbCO fits excellently the linear correlation, implying that, very probably, ruffling distortion of the heme is responsible for this relationship. Indeed, with the inclusion of MbCO, the correlation coefficient increases to 0.945. Nevertheless, further investigations are needed with heme proteins of known three-dimensional structure in an effort to elucidate whether ^{57}Fe NMR shieldings can be used in structure refinement protocols for the extraction of more accurate structures for heme rings in proteins.

Recently, we showed the great potential of the shieldings of meso carbons in structural studies of porphyrin distortion in superstructured iron heme model compounds in solution.⁸ When the average shieldings of the meso carbons, $\delta(^{13}\text{C}_{m,\text{av}})$ (ppm), for a variety of TPP derivatives are plotted against the absolute crystallographic average displacement of the C_{meso} atoms relative to the porphyrin core mean plane, $|C_m|$ (Å), an excellent linear correlation is observed. When $\delta(^{13}\text{C}_{m,\text{av}})$ is plotted against $\delta(^{57}\text{Fe})$ for the CO adducts of the heme model compounds of

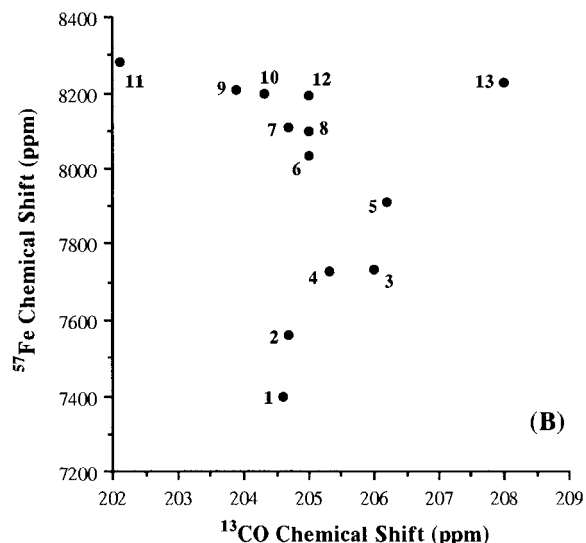
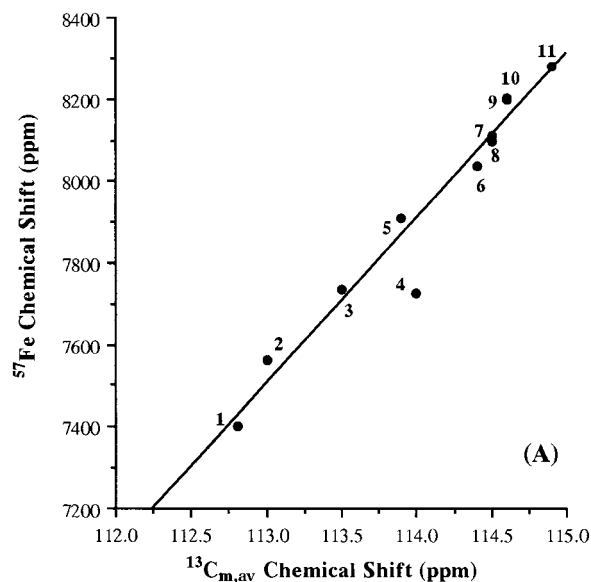


Figure 4. (A) Plot of $\delta(^{57}\text{Fe})$ (ppm) vs $\delta(^{13}\text{C}_{m,\text{av}})$ (ppm) for the heme model compounds of Figure 1. (B) Plot of $\delta(^{57}\text{Fe})$ (ppm) vs $\delta(^{13}\text{CO})$ (ppm) for the heme model compounds of Figure 1. Data points are as follows: 1, D α -atropisomer; 2, D β -atropisomer; 3, C α -atropisomer; 4, B; 5, C β -atropisomer; 6, A; 7, F(1-Bulm); 8, F(1,2-diMeIm); 9, G conformer 1; 10, G conformer 2; 11, E; 12, H; 13, Mb.

Figure 1, an excellent linear correlation is also observed (Figure 4A), which can be expressed as

$$\delta(^{57}\text{Fe}) \text{ (ppm)} = -3.828 \times 10^4 + 405.18\delta(^{13}\text{C}_{m,\text{av}}) \text{ (ppm)} \quad (2)$$

with a correlation coefficient of 0.956. This relationship is of great importance since it is useful for detecting possible errors in reported ^{57}Fe shieldings and for predicting the chemical shift for a given superstructured iron(II) porphyrinate complex.²¹ This correlation has significant advantages compared to the rough correlation between Mössbauer quadrupolar splittings and ^{57}Fe shieldings.^{10a}

(21) $\delta(^{13}\text{C}_m)$ of the meso carbons of the TPP(1-MeIm)CO complex is strongly deshielded by ~ 4 ppm compared with those of the amide and other type superstructured TPP derivatives, which can be rationalized in terms of substituent increments of ^{13}C shieldings: Breitmaier, E.; Voelter, W. *Carbon-13 NMR Spectroscopy*, 3rd ed.; VCH: Weinheim, Germany, 1990.

Interestingly, the ^{57}Fe shielding difference between the α - and β -atropisomers is very large, being 160 and 176 ppm for PocPiv and Piv₂C₈, respectively. This means that atropisomerization may cause large variations in the degree of porphyrin ruffling. Equation 1 can be used to extract the difference in the degree of ruffling between α - and β -atropisomers, which is 0.12 Å for PocPiv (**D**) and 0.14 Å for Piv₂C₈ (**C**). This result is of significance because there is always a mixture of α - and β -atropisomers in the solution of the above-mentioned models, due to the heating required for iron insertion. Therefore, kinetic and thermodynamic data for heme models, as average values, cannot be directly correlated with X-ray structural data.

Several workers have demonstrated that the ^{13}C shieldings of the Fe–C–O unit, $\delta(^{13}\text{CO})$, of heme proteins and synthetic model compounds in solution vary widely, and excellent correlations were found with the infrared C–O vibrational frequencies, $\nu(\text{C–O})$.²² It was suggested that both $\delta(^{13}\text{CO})$ and $\nu(\text{C–O})$ reflect similar interactions which are primarily the modulations of π back-bonding from the Fe $d\pi$ to the CO π^* orbital by the distal pocket polar interactions. A plot of $\delta(^{13}\text{CO})$ against $\delta(^{57}\text{Fe})$ for the model compounds of Figure 1 indicates the lack of correlation (Figure 4B) (correlation coefficient is only 0.018). This demonstrates that $\delta(^{57}\text{Fe})$, in contrast to $\delta(^{13}\text{CO})$, is not influenced by polar interactions of bound CO with distal residues.

(22) (a) Moon, R. B.; Dill, K.; Richards, J. H. *Biochemistry* **1977**, *16*, 221–228. (b) Satterlee, J. D. *Inorg. Chim. Acta* **1983**, *79*, 170–172. (c) Potter, W. T.; Hazzard, J. H.; Choc, M. J.; Tucker, M. P.; Caughey, W. S. *Biochemistry* **1990**, *29*, 6283–6295. (d) Park, K. D.; Guo, K.; Adebodun, F.; Chiu, M. L.; Sligar, S. G.; Oldfield, E. *Biochemistry* **1991**, *30*, 2333–2347. (e) Kalodimos, C. G.; Gerotheranassis, I. P.; Troganis, A.; Loock, B.; Momenteau, M. J. *Biomol. NMR* **1998**, *11*, 423–435. (f) Kalodimos, C. G.; Gerotheranassis, I. P.; Hawkes, G. E. *Biospectroscopy* **1998**, *4*, S57–S69.

Conclusion

The results we have presented above unambiguously show the great potential of ^{57}Fe shieldings as a quantitative tool in structural studies of heme model compounds. $\delta(^{57}\text{Fe})$ compares favorably with other NMR parameters, notably NOEs, scalar J coupling constants, and relaxation times currently being used for studies of biomolecular structures and dynamics in solution. The present direct relationship between heme ruffling and ^{57}Fe shieldings provides the needed framework for the inclusion of $\delta(^{57}\text{Fe})$ in NMR structure refinement protocols for the extraction of more accurate structures for heme rings in hexacoordinated carbonmonoxy heme models in solution. Furthermore, our findings emphasize the value in predicting ^{57}Fe chemical shifts in metalloporphyrins from ^{13}C chemical shifts of the meso carbons of the TPP derivatives. Further investigations of synthetic model compounds and particularly heme proteins, where the uncertainty in determining the X-ray structures is high,²³ are currently in progress.

Acknowledgment. This research was supported by the Greek General Secretariat of Research and Technology, the Greek Scholarship Foundation (Ph.D research fellowship to C.G.K.), and EMBO (Short Term Fellowship to C.G.K.). We wish to thank the ULIRS Bruker AMX-600 facility located at QMC and the EU-Large Scale PARABIO Facility at the University of Florence for the use of the Bruker AMX-600 and AVANCE-600 instruments, respectively.

JA983889G

(23) Absolute values of positional uncertainties are the subject of much debate but could be estimated to be 0.1 to ~0.2 Å at 2 Å resolution.